Optik - International Journal for Light and Electron Optics 264 (2022) 169455

Contents lists available at ScienceDirect

Optik

journal homepage: www.elsevier.com/locate/ijleo

Original research article

High-power narrow-linewidth 780 nm diode laser based on external cavity feedback technology of volume Bragg grating

Jinliang Han [a,b], Jun Zhang [a,*], Xiaonan Shan [a], Yawei Zhang [a], Hangyu Peng [a], Li Qin [a], Lijun Wang [a]

[a] Changchun Institute of Optics, Fine Mechanics and Physics, Chinese Academy of Sciences, Changchun 130033, China
[b] University of Chinese Academy of Sciences, Beijing 100049, China

ARTICLE INFO

Keywords:
DPAL
Diode laser
External cavity feedback
Narrow linewidth
Metal ceramic heater

ABSTRACT

A diode-pumped alkali metal vapor laser (DPAL) combines the advantages of a solid laser and a gas laser. DPAL is useful in the industrial, medical, aerospace and military fields and can yield high output power while maintaining excellent beam quality. However, applications in many fields are limited due to the narrow absorption spectrum of the alkali metal vapor laser. In this study, a novel linewidth narrowing structure of the high-power diode laser based on volume Bragg gratings (VBGs) is proposed to match the absorption spectrum of the alkali metal vapor laser. With the combination of fast-axis collimating lens, beam transformation systems, slow-axis collimating lens, VBGs and metal ceramic heaters, the divergence angles of both fast and slow axis are compressed within 10 mrad. A high-power narrow linewidth diode laser source with a central wavelength of 780.044 nm, a spectral width of 0.138 nm, and an output power of 1090 W is achieved at an operating current of 50 A. Experimental results show that the effect of external cavity feedback based on VBG is improved and the multi-channel spectral linewidth is narrowed effectively by such a structure. The diode laser source based on this structure can be applied for pumping the rubidium alkali metal vapor laser.

1. Introduction

In recent years, alkali metal vapor lasers pumped by diode lasers have attracted extensive attention [1–5]. This type of laser combines the advantages of diode laser that has high efficiency, small size, and good reliability, and those of solid-state and gas lasers that have high quantum efficiency, excellent gas-medium circulating cooling, and efficient near-infrared atomic spectrum atmospheric transmissivity. Alkali metal vapor lasers can be widely utilized in the industrial processing, medical treatment, aerospace, and military fields [6–9]. At present, diode-pumped alkali metal vapor laser (DPAL) with high power is still under development. The pump source with high performance, as one of the key technical bottlenecks, is an important factor that restricts development.

To achieve efficient pumping of DPAL, the diode laser pump source must have the following characteristics: (i) It has to improve the beam quality of the diode laser and scale the output power by beam combination technology [10]. (ii) The stable spectrum and narrow spectral linewidth have to match the absorption spectrum of the alkali metal vapor laser [11]. The typical spectral linewidth of commercial diode lasers as pump sources is usually 2–5 nm, and the alkali metal vapor laser absorption spectrum is extremely narrow, which leads to a mismatch between the pump and absorption spectra [12]. To solve these problems, on the one hand, buffer gas such as

* Corresponding author.
E-mail address: zhangjciomp@163.com (J. Zhang).

https://doi.org/10.1016/j.ijleo.2022.169455
Received 16 February 2022; Received in revised form 7 May 2022; Accepted 6 June 2022
Available online 8 June 2022

helium should be flushed into the alkali metal vapor cell to widen the absorption spectrum of alkali metal atoms by collision. On the other hand, concave gratings or volume Bragg gratings (VBGs) are used to narrow the spectral linewidth of the diode laser through external cavity feedback technology [13–15].

Over the past years, several research communities have investigated the high power narrow-linewidth diode laser pumping source. Yang Zining et al. reported that an 80 W laser diode array with 0.1 nm linewidth and 780 nm central wavelength was realized through external cavity technology of volume Bragg grating (VBG). It can be used for Rubidium vapor laser pumping [16]. Rajiv Pandey et al. reported that the diode laser with output power of 100 W/bar and spectral linewidth of 0.06 nm was realized basing on a micro-channel water-cooled stack with collimation in both-axes and VBG external cavity feedback [17]. Rui Wang et al. reported a VBG coupled diode laser module operating at 811.53 nm suitable for metastable argon atoms pumping. The maximum output power was more than 100 W with 4.6% power loss compared to the free-running. The linewidth of the emission spectrum was 0.15 nm with a tunable range of 200 pm [18]. The conventional external cavity structure includes a fast axis collimation lens, a slow axis collimation lens, and a VBG. However, VBG has angle selectivity. After the fast and slow axes collimation, the divergence angle of the slow axis still reaches 20–50 mrad, and then affects the external cavity feedback effect.

Starting from the bottleneck of DPAL pump source technology, in this paper, we present a novel structure that uses the combination of fast-axis collimators (FACs), beam transformation systems (BTSs), slow axis collimators (SACs), and VBGs to decrease the divergence of laser radiated on the VBGs for linewidth narrowing, the divergence angle of fast and slow axes can be reduced to 10 mrad. Using metal ceramic heater (MCH) to heat the VBGs for spectral stabilization and control, the multi-channel laser bars can achieve temperature control independently. The narrow linewidth diode laser source producing 1090 W power is realized using the beam space combination technology. The central wavelength is 780.044 nm and the spectral width is 0.138 nm. Such a diode laser can be applied to pump the rubidium alkali metal vapor laser and thus lays the technical foundation for the efficient pumping of DPAL.

2. Experimental design and simulation

2.1. Tunable external cavity feedback

The external cavity feedback diode laser is mainly composed of laser chips, a shaping lens group, and a laser feedback element. The diode laser at free running is collimated by a shaping lens group and radiates to the feedback element, which can select the mode of the incident laser and realize the optical feedback. Only the eligible laser returns to the laser chip and couples into the internal laser field. The wavelength tuning and linewidth narrowing can be further ensured by adjusting the feedback element [19].

Fig. 1 shows the structure diagram of the external cavity feedback diode laser. The reflectivity of the rear cavity surface of the diode laser chip is defined as r_1, the front cavity surface is r_2, the diffraction efficiency of VBG is r_3, and the resonant cavity length in the active region and outer cavity length are represented by l and L, respectively.

The spectral linewidth formula of the external cavity feedback diode laser can be expressed as [20].

$$\Delta\nu = \frac{\Delta\nu_0}{\left[1+\sqrt{1+\alpha^2}\,R\cos\Delta\varphi\right]^2} \tag{1}$$

where $\Delta\nu_0$is the spectral linewidth of diode laser operating freely without external cavity feedback, $\alpha$is the linewidth expansion factor, and $R$is the external cavity feedback factor. $\Delta\varphi = \varphi_0 - \tan^{-1}\alpha$, and in the case of the phase matching, we can obtain$\cos\Delta\varphi = 1$. The expression of the narrowest linewidth with the external cavity feedback can be obtained as

$$\Delta\nu = \frac{\Delta\nu_0}{\left[1+\sqrt{1+\alpha^2}\,R\right]^2} \tag{2}$$

The external cavity feedback factor R can be expressed as:

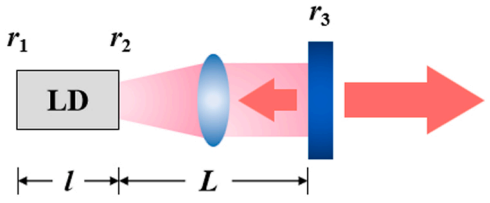

Fig. 1. Schematic of external cavity diode laser.

$$\begin{cases} \mathrm{R} = \dfrac{1 - r_2^2}{r_2} r^3 \dfrac{\tau}{\tau_{in}} \\ \tau = \dfrac{2L}{c} \\ \tau_{in} = \dfrac{2nl}{c} \end{cases} \tag{3}$$

where $\tau$is the external cavity roundtrip time, and τ_{in} is the internal cavity roundtrip time. An approximate expansion of the preceding linewidth expression can be obtained as

$$\Delta\nu = \Delta\nu_0 \left(1 + \alpha^2\right)^{-1} \left(\frac{1 - r_2^2}{r_2}\right)^{-2} r_3^{-2} (nl)^2 L^{-2}. \tag{4}$$

Through Eq. (4), we find that the narrowed linewidth of the external cavity feedback diode laser is inversely proportional to the diffraction efficiency ${r_3}^2$, inversely proportional to the growth of the external cavity L^2, and proportional to the reflectivity of the front cavity surface ${r_2}^2$. Therefore, we need to improve the diffraction efficiency of VBG and reduce the reflectivity of the front cavity surface of the laser chip to obtain the narrow linewidth of the diode laser.

However, catastrophic optical mirror damage (COMD) can easily occur when the reflection efficiency of the front cavity surface is decreased and the diffraction efficiency of VBG is increased. On the one hand, the lower the reflectivity of the front cavity surface of the laser chip is, the more likely it is to be affected by the external cavity feedback, which leads to an increase in the laser power density at the local position of the front cavity surface, and then accelerates the damage of the front cavity surface. On the other hand, increasing the diffraction efficiency of VBG causes peaks of laser power on the cavity surface, resulting in COMD [21]. Accordingly, the reflectivity of the front cavity surface and the diffraction efficiency of VBG should be optimally designed to obtain the fine reliability and spectral locking of the laser chip.

2.2. Beam-shaping design

Typical divergence angles of the diode laser in fast (30–60°) and slow (8–12°) axis are so large that it is necessary to collimate the laser beam by using a collimator firstly [22,23]. In this study, a combination of a FAC, a BTS, and a SAC as a collimation system is used to shape spots and reduce divergence angles in fast and slow axis.

As shown in Fig. 2, we use a FAC and a BTS with a focal length of 0.41 mm. The technical parameters of BTS are shown in Table 1. Through BTS, the rotation angle of beam spot is 90°. The divergence angle of the fast axis after the collimation system is 4.2 mrad (95%), which is simulated by Zemax optical design software, as shown in Fig. 3. In the packaging process of the laser bar, the stress generated by welding can cause a “smile” effect, which results in a larger divergence angle after the alignment of the fast axis. Therefore, the divergence angle of the fast axis is defined as 8 mrad for the subsequent design of the beam combination.

Beam spots in the fast and slow axis can be exchanged by BTS. Therefore, the collimation of the slow axis can be realized by a single flat convex cylindrical lens. The divergence angle after collimation is determined by the focal length of SAC, which is expressed as

$$f_{SA}{}' = \frac{\omega_{SA}}{2\tan(\theta_{SA}{}'/2)}, \tag{5}$$

where ω_{SA}= 150 μm is the width of laser chip, and $\theta_{SA}{}'$ is the slow axis divergence angle after collimation. What after collimationen divergence angles in the fast and slow axis are the same, the focal spot is closely symmetrical. Therefore, the slow axis divergence angle after collimation is set to 8 mrad, and the required focal length of SAC $f_{SA}{}'$ can be set to 18.75 mm through calculation.

In addition, the size of beam spot after collimation in the slow axis is also considered. Theoretically, the divergence angle in slow

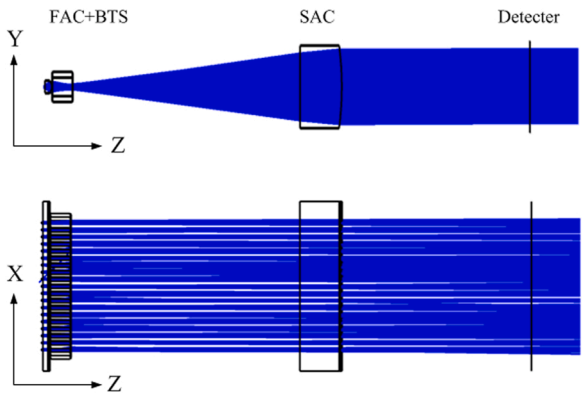

Fig. 2. Simulation diagram based on FAC+BTS+SAC collimation structure.

Table 1
Typical parameters of BTS.

Parameters	Unit	Specifications
Material		S-NPH3 / S-TIH53 (Ohara)
Length	mm	11.5 ± 0.1
Width	mm	1.5 ± 0.1
Thickness	mm	2.15 ± 0.1
Pitch	mm	0.5
Transmission	%	≥ 98
Focal length	mm	0.41

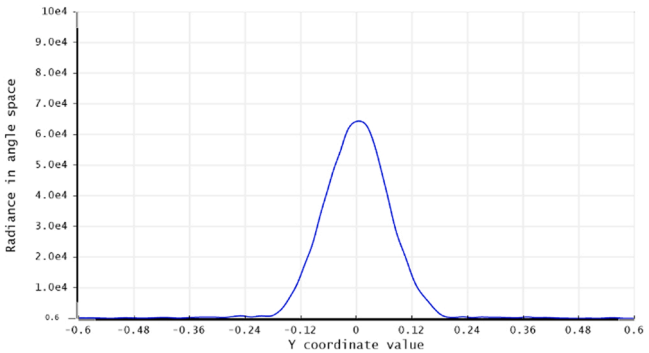

Fig. 3. Simulation results of fast axis divergence angle.

axis can be infinitely small, but when the divergence angle decreases, the size of beam spot increases, which is not conducive to the beam combination. Therefore, the divergence angle and beam spot size should be considered. The size of the beam spot in the slow axis after collimation $\omega_{SA}{}'$ is determined as follows:

$$\omega_{SA}{}' = 2f_{SA}{}' \tan(\theta_{SA}/2). \tag{6}$$

Through calculation, $\omega_{SA}{}'$ is 3.26 mm when slow axis divergence angle before collimation θ_{SA} is 10°. We simulate the divergence angle and beam spot size in slow axis behind SAC. The simulation results are compatible with the theoretical calculation values. The divergence angle after collimation in slow axis is 8.05 mrad, and the size of the beam spot is 3.2 mm. (Fig. 4).

The effect of external cavity feedback can be improved effectively by collimating the beam in the fast and slow axis and compressing the divergence angle radiated on the VBG. Compared with the conventional FAC + SAC + VBG structure, our proposed structure uses a BTS after FAC for exchanging the spot size in the fast and slow axis, which can reduce the divergence angle in the slow axis in the subsequent beam shaping. The external cavity feedback structure with added BTS is shown in Fig. 5.

The diffraction wavelength of VBG becomes unstable due to its own temperature. The different power of laser radiated on the VBG can cause different temperatures of VBG. Furthermore, a certain amount of error occurs in its diffraction wavelength during production. Thus, the temperature of VBGs should be controlled to obtain consistent spectral characteristics [24]. We propose to replace the conventional TEC with MCH. On the one hand, the hot side of TEC needs effective heat dissipation, which requires the design structure to be close to the laser shell. Such a structure is highly complex and not conducive to miniaturization design. On the other hand, TEC is usually suitable for heating in the middle- and low-temperature range, and the temperature of the hot side should be not more than 60 ℃. Thus, the small tunable temperature range is unsuitable for controlling the diffraction wavelength of VBG. (Fig. 6).

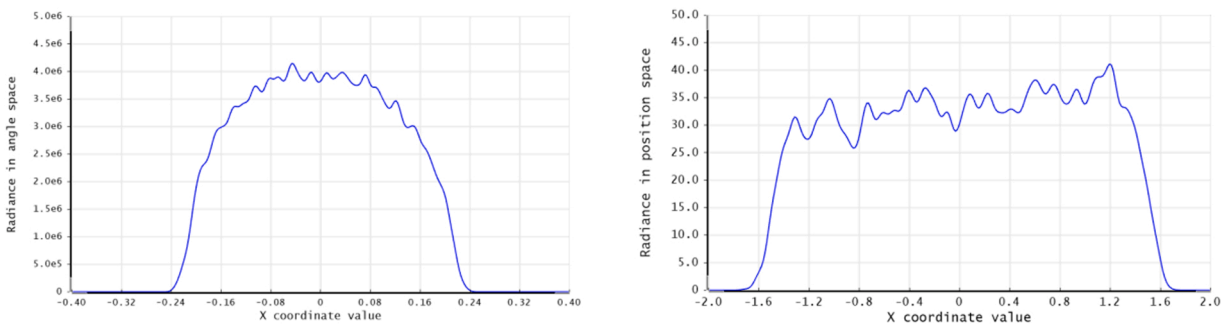

Fig. 4. Simulation results of slow axis divergence angle and beam spot size.

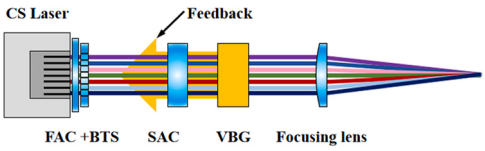

Fig. 5. Schematic of external cavity feedback structure based on VBG.

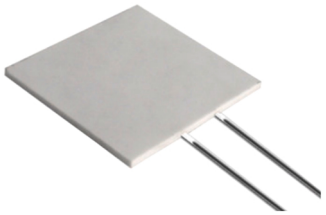

Fig. 6. Picture of MCH.

To scale output power, optical stacking and beam spatial combining technology are employed. The optical design of the high-power narrow linewidth diode laser is adopted as shown in Fig. 7(a). Three beam groups are designed in fast axis, that is, X-axis. The spot size of each bar is approximately 10 mm in the fast axis, so the stacking spot size of three groups is 30 mm. Eight laser bars are placed in slow axis, that is, Y-axis. These laser bars are mounted on the mechanical ladder heatsink. The spot size of a single laser bar in slow axis is 3.2 mm, and the stacking spot size of eight laser bars is 25.6 mm. Considering the optical path and light blocking of the mechanical ladder structure, the distance between three beam spots in the X-axis is set to 1 mm, so the overall size of the spot is 32 mm. The step gap in the Y-axis is designed to 4 mm, and then the overall spot size is 32 mm, which finally achieves the purpose of beam shaping. The simulated spot diagram of the beam combination is shown in Fig. 7(b).

3. Experimental results and analysis

3.1. External cavity feedback of single laser bar

The external cavity feedback of the single 780 nm diode laser bar is studied. The reflectivity of the front facet of the laser chip R_{ff} is set to 2–3%. The size of VBG with a center wavelength of 779.8 ± 0.1 nm is 12 mm × 1.5 mm × 3 mm. The testing structure is built as shown in Fig. 8.

The diffraction efficiency of VBG is set to 5%, 10%, and 15%, respectively. Fig. 9 shows the output power under free running and external cavity feedback as a function of operating current. As shown in Fig. 9, the power curve has minimal difference under different diffraction efficiencies of VBG. With the increase of diffraction efficiency, the power after external cavity feedback shows a trend of slight decline, but the difference is less than 1 W. This condition indicates that VBGs with diffraction efficiency from 5% to 15% are suitable for external cavity feedback, and the power difference is negligible.

In addition to the output power after external cavity feedback, the central wavelength and spectral linewidth should also be

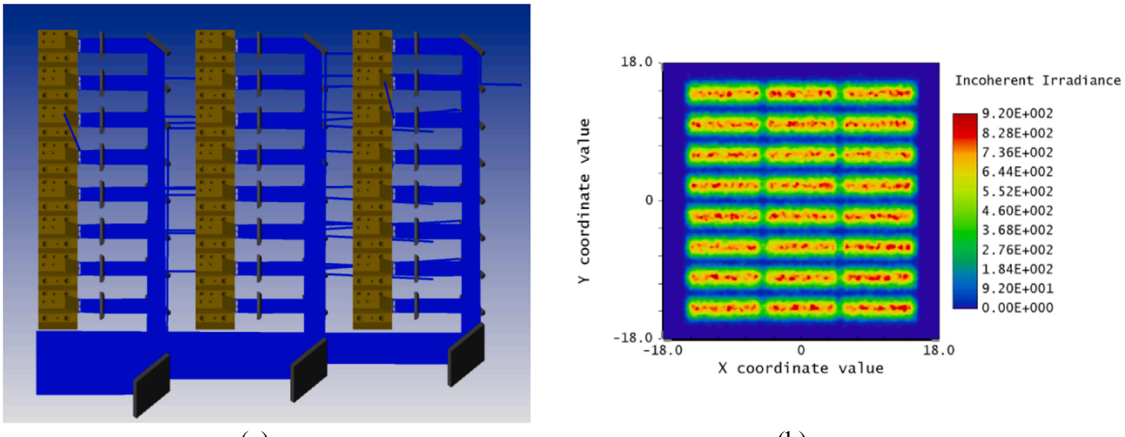

Fig. 7. (a) Optical design of high-power narrow linewidth diode laser. (b) Simulated spot diagram of beam combination.

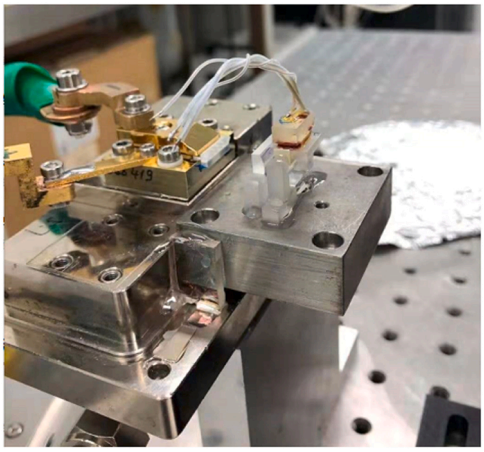

Fig. 8. Testing diagram of single bar.

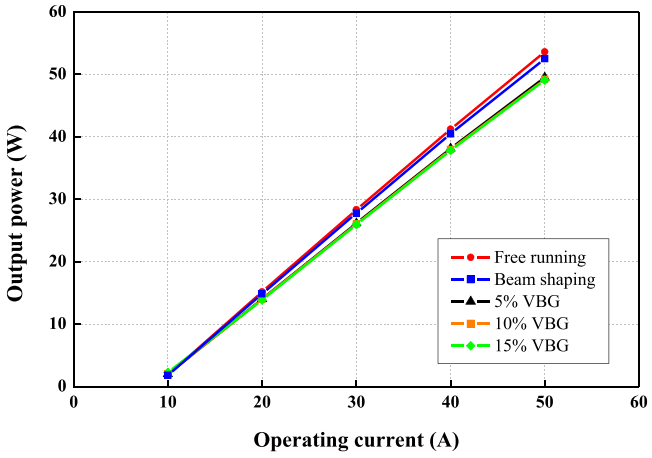

Fig. 9. Output power as a function operating current of single bar with and without external cavity feedback.

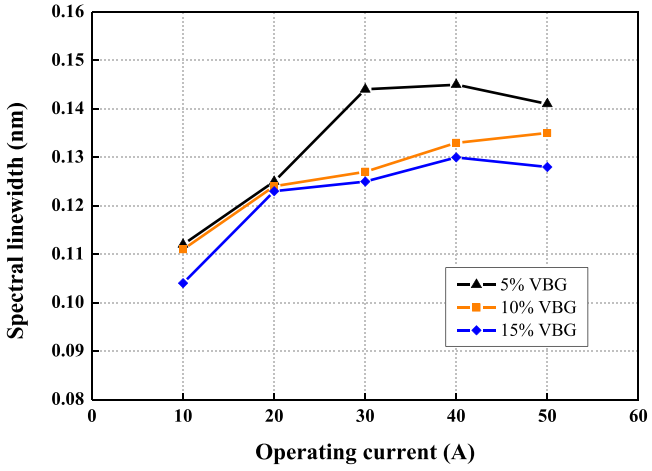

Fig. 10. Spectral linewidth of single bar as a function of operating current for different VBG diffraction efficiencies.

considered. Fig. 10 shows the locked spectral linewidth (FWHM) with different diffraction efficiency of VBGs at the operating current of 10–50 A. Results demonstrate that the spectral linewidths are relatively small and close at low operating current, but the spectral linewidth increases as the operating current increases. Among three different diffraction efficiencies of VBGs, the locked spectral linewidth narrows as the diffraction efficiency increases, which is also consistent with the theoretical analysis results provided.

Fig. 11 shows the central wavelength of VBG as a function of operating current for three diffraction efficiencies of VBG. Experimental results indicate that the shift of the central wavelength decreases to 0.003 nm/A. VBGs with diffraction efficiency from 5% to 15% can meet design requirements. However, low diffraction efficiency of VBG causes a small amount of laser feedback to the active area of the diode laser, which increases the instability of external cavity locking when multiple external cavity locking is performed. Given all that, VBG with diffraction efficiency of 15% is selected for the diode laser pump source designed in this study.

According to Eq. (4), the linewidth of external cavity feedback diode laser is inversely proportional to the square of the cavity length. Fig. 12 shows the spectral linewidth as a function of operating current. VBG with diffraction efficiency of 15% is used for cavity feedback based on the single bar. The distances between VBG and SAC are set to 5, 10, 15, 20, and 25 mm. The spectral linewidth does not change significantly as the cavity length increases. Thus, changing the cavity length is not an effective way to narrow the spectral linewidth. This result occurs mainly because the change of cavity length has obvious influence on the single-mode laser, while the high power diode laser has multi-mode output, so the spectral linewidth does not change significantly. In addition, due to the angle selectivity of VBG, with the increase of the cavity length, part of the laser cannot return to the laser chip for mode competition after the feedback of external cavity, which will lead to the linewidth broadening. In this case, the phenomenon of laser self-excitation is prone to occur, and the laser output of multi-center wavelength is formed.

Through the collimation of the traditional structure of FAC + SAC + VBG, the divergence angle after SAC is 42 mrad, which is larger than the effective feedback angle of VBG (17.5 mrad). Owing to the angle selectivity of VBG, when the divergence angle of the laser radiated to VBG is large, the increased cavity length causes that part of the feedback laser to be unable to return to the active region of the diode laser for mode competition. Thus, part of the laser produces a self-excitation effect that influences the effect of external cavity feedback, as shown in Fig. 13(a). In this study, a structure of FAC + BTS + SAC + VBG is proposed for beam collimation, which can decrease divergence angles in the fast and slow axis to 10 mrad level simultaneously. The increased cavity length does not affect the spectral stability, as shown in Fig. 13(b). Furthermore, the shorter cavity length is more conducive to the compact design of the optical system.

According to the expression of spectral linewidth expansion, the spectral linewidth of the diode laser with external cavity feedback is proportional to the reflectivity of the laser chip output surface. Ideally, the laser chip with low front cavity reflectivity is more advantageous to narrow the linewidth. Diode laser chips with the same structural parameters are selected, and the reflectivity of front facet R_{ff} is 0.5% as an example. The spectral linewidth and central wavelength as a function of operating current under different diffraction efficiencies are shown in Fig. 14. Compared with Fig. 10, the spectral linewidth is narrowed significantly, which is consistent with the theoretical analysis. However, the smaller the reflectivity of the front cavity surface is, the more easily the external cavity feedback is affected. The increased local power density of the front cavity surface causes an acceleration in the cavity surface damage and COMD. The threshold current of the laser chip with low AR coating is 15.5 A, but it is only 8.8 A with normal AR coating. Therefore, the laser chip with normal coating is used in the subsequent laser design.

3.2. *High-power narrow linewidth diode laser pump source*

A photograph of the 780 nm kW class narrow linewidth diode laser pump source is shown in Fig. 15. Due to the different initial central wavelengths and spectral linewidths of different laser bars, eight laser bars from the same channel are taken as an example for analysis and discussion. The spectra under free running at 50 A are shown in Fig. 16(a). When the multichannel lasers are beam combined, the central wavelength range and overall spectral linewidth are large, and therefore cannot meet the requirements of DPAL pumping.

The spectra of eight laser bars based on VBG without temperature control are measured as shown in Fig. 16 (b). After external cavity feedback, the central wavelength can be controlled within the range of VBG diffraction wavelength, and the linewidth of the single bar can be narrowed to near 0.1 nm. However, due to the manufacturing tolerance of VBG, the central wavelengths of eight laser bars do not coincide completely after the multiplexing beam. In the meantime, after working for a long time, the differences in heat accumulation between VBGs further lead to different shifts of central wavelengths, thus affecting the overall spectral linewidth.

To solve the aforementioned problems, MCH is mounted under VBG to control the temperature of the latter. According to the temperature and wavelength shift characteristics of VBG, the selected VBG diffraction center wavelength is slightly lower than 780 nm, and the feedback wavelength is locked to 780 nm by increasing the temperature. The temperatures of VBGs in 24 channels are controlled accurately and independently. The optimal combination of spectral linewidth can be achieved by adjusting the heating temperature of MCHs when working with high power for a long time. The interface of temperature control is shown in Fig. 17.

By measuring the central wavelength and spectral linewidth of each channel VBG, we can set the temperature of each channel MCH so that the central wavelengths of all 24 channels can effectively coincide. The spectra after controlling the temperature of VBGs are measured as shown in Fig. 18. When the temperature of MCH is set to 50 ℃, each MCH is adjusted according to the wavelength feedback. The overall central wavelength of the diode laser pump source is 780.044 nm and the spectral linewidth is 0.138 nm.

A CW power of 1090 W and an E–O efficiency of 48.91% are measured at the operating current of 50 A (Fig. 19). The external cavity feedback efficiency of the diode laser pump source is 90.08%. When the water-cooling temperature is 20 ℃, the output power under free running is 1286 W at 50 A. After collimation and space beam combination, the output power is 1210 W, and the optical–optical (O–O) efficiency is 94.09%. The final O–O efficiency of the diode laser pump source is 84.76%, which is defined as the ratio

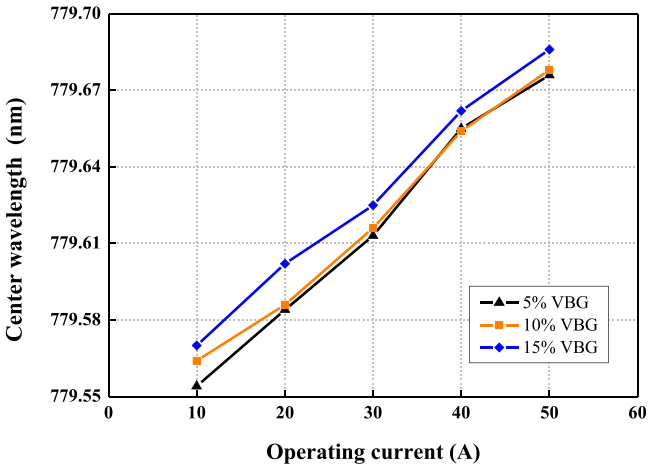

Fig. 11. Center wavelength of single bar as a function operating current for different VBG diffraction efficiencies.

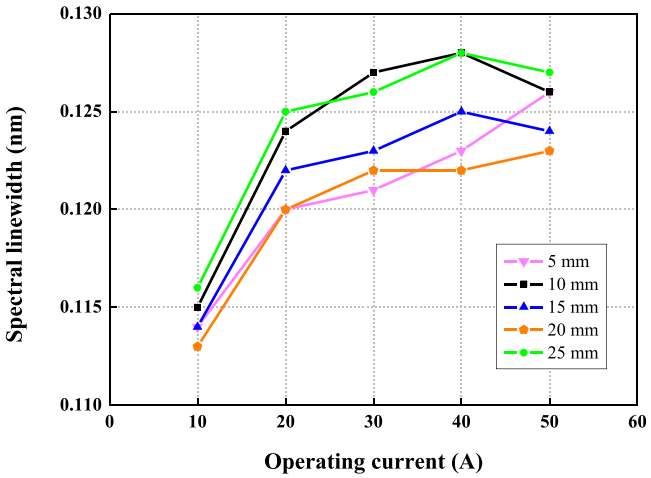

Fig. 12. Spectral linewidth of single bar as a function of operating current for different cavity lengths.

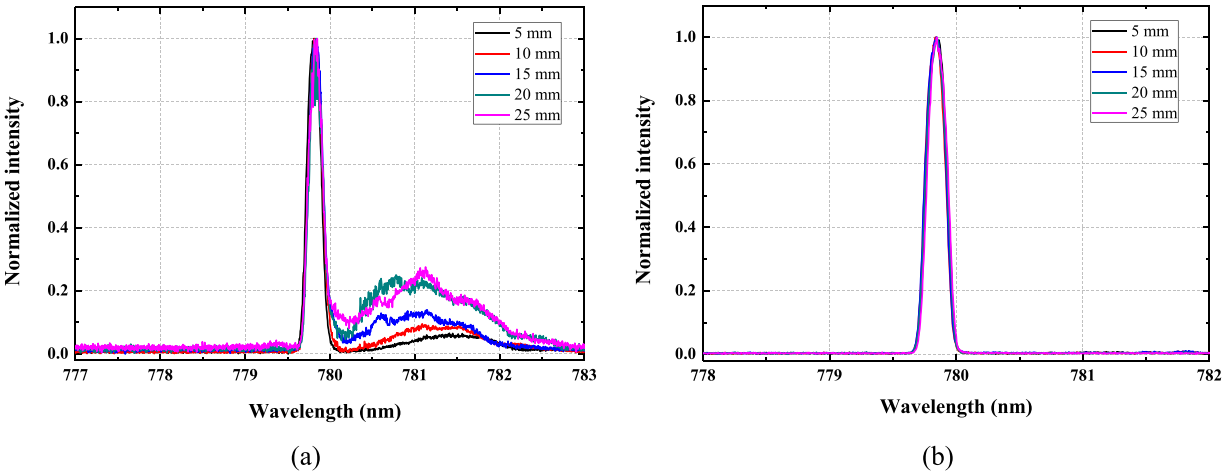

Fig. 13. Locking spectrum of single bar by (a) FAC + SAC + VBG (b) FAC + BTS + SAC + VBG for different cavity lengths.

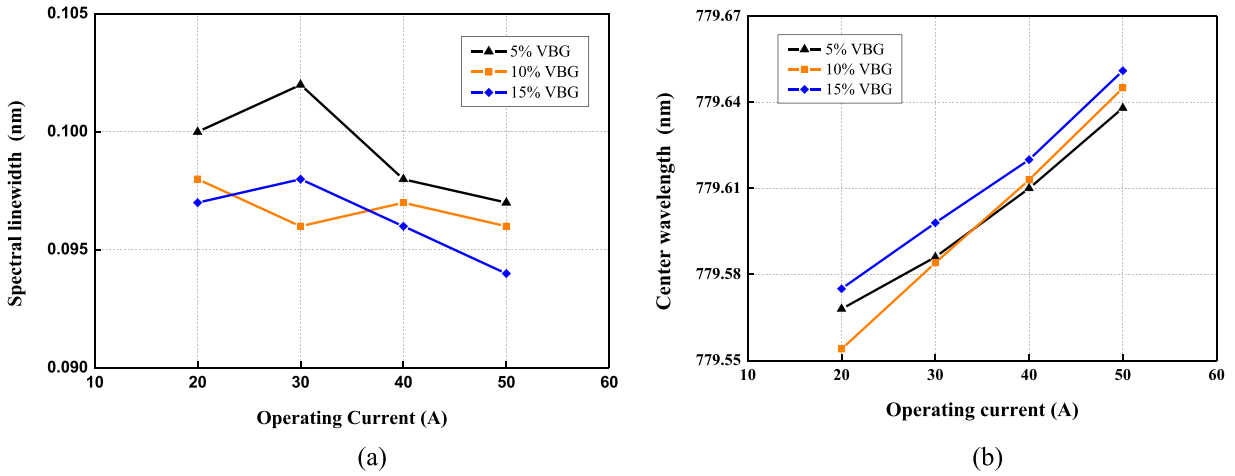

Fig. 14. (a) Spectral linewidth and (b) center wavelength of single bar ($R_{ff} = 0.5\%$) as a function of operating current for different VBG diffraction efficiencies.

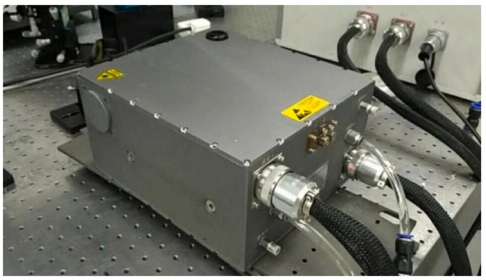

Fig. 15. Photograph of 780 nm kW class narrow linewidth diode laser source.

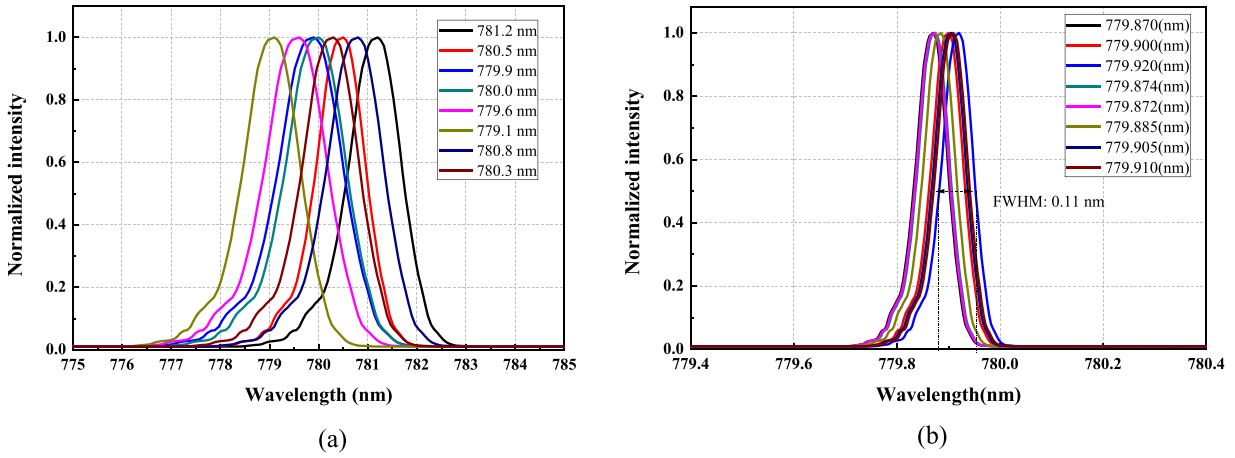

Fig. 16. Spectrum of eight laser bars at 50 A (a) under free running and (b) with external cavity feedback.

of the output power after external cavity feedback to the total power under free running.

To obtain the effect of MCH temperature on the central wavelength of the diode laser pump source, we measure the spectrum under different MCH temperatures, as shown in Fig. 20. The MCH temperature is set to 40, 50, and 60 ℃. The increased MCH temperature results in a red shift in the center wavelength of the diode laser pump source. The temperature drift is 7.45 pm/℃, so the central wavelength can be finetuned by controlling the MCH temperature.

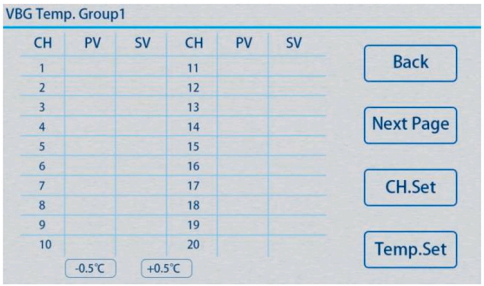

Fig. 17. Temperature control interface. CH represents channel , PV represents practical temperature , and SV represents setting temperature.

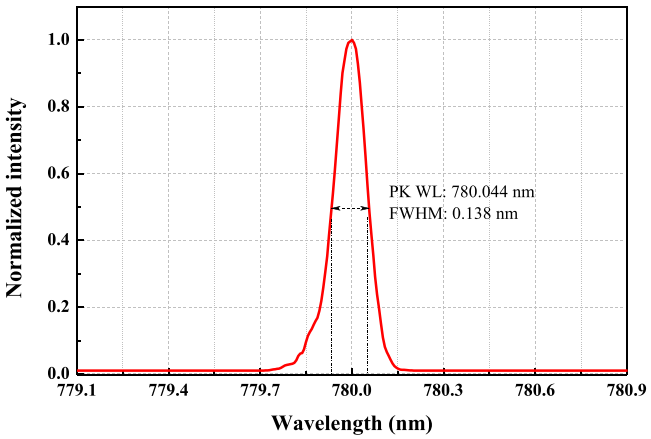

Fig. 18. Spectrum of diode laser pump laser with external cavity feedback under MCH temperature of 50 ℃.

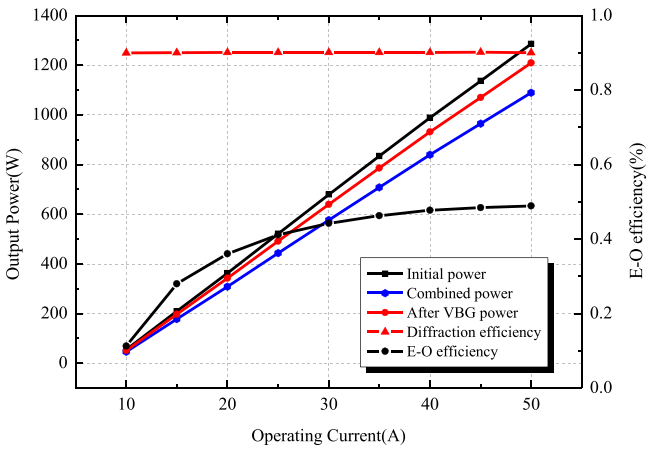

Fig. 19. Output power and E–O efficiency as a function of operating current.

4. Conclusion

In this study, a novel linewidth narrowing structure of a high-power diode laser based on volume Bragg gratings is proposed. Such a structure consists of a fast-axis collimating lens, a beam transformation system, a slow-axis collimating lens, a VBG, and a MCH. Decreasing the divergence of the laser radiated on the VBG can improve the effect of external cavity feedback, and heating VBGs individually is realized by MCHs to lock and control multiple-channel wavelengths. By studying the impact of VBG diffraction efficiency, external cavity length, and reflectivity of the front cavity surface of the laser chip on spectral narrowing and wavelength locking, we obtained the optimal parameters of external cavity feedback based on theoretical design. A kW class high power and narrow linewidth diode laser with central wavelength of 780.044 nm, spectral width of 0.138 nm, and output power of 1090 W is

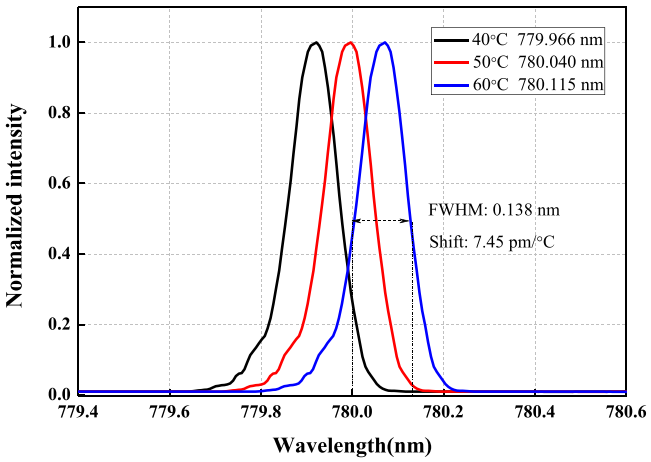

Fig. 20. Spectrum at operating current of 50 A under different temperatures of MCH.

developed, which can be used to pump rubidium metal vapor lasers. Further research is needed to scale the output power and develop a diode-laser pump source with output power of 10 kW, narrow linewidth, miniaturization, and high E–O efficiency, so that an advanced laser pump source will be available for the industrial, medical, aerospace, and military fields.

Funding

This work was supported by the Natural National Science Foundation of China (NSFC) (61991433, 62121005), Pilot Project of CAS (XDB43030302), Equipment Pre Research (2006ZYGG0304, 2020-JCJQ-ZD-245–11), Key Research and Development Project of Guangdong Province (2020B090922003).

Declaration of Competing Interest

The authors declare that they have no known competing financial interests or personal relationships that could have appeared to influence the work reported in this paper.

Acknowledgment

We thank our project partners for the assistance and fruitful discussions.

References

[1] R. Luzon, S. Kostyukovets, I. Auslender, N. Mayorkas, E. Yacoby, B.D. Barmashenk, S. Rosenwaks, Improving the beam quality of DPALs by refractive index gradients induced by the pump beam in the heated gain medium: experimental verification of the theoretical prediction, J. Opt. Soc. Am. B 38 (2) (2021) 550–552.
[2] I. Auslender, E. Yacoby, B.D. Bramashenko, S. Rosenwaks, General model of DPAL output power and beam quality dependence on pump beam parameters: experimental and theoretical studies, J. Opt. Soc. Am. B 35 (12) (2018) 3134–3142.
[3] B. Shen, X. Xu, C. Xia, B. Pan, Three-dimensional kinetic and fluid dynamic modeling and three iterative algorithms for side-pumped alkali vapor lasers, Opt. Commun. 402 (2017) 593–599.
[4] C. Xia, J. Huang, C. Su, X. Xu, B. Pan, Theoretical research of time dependent pulsed diode-pumped Rb vapor laser, Opt. Laser Technol. 133 (2021), 106529.
[5] B.V. Zhdanov, T. Ehrenreich, R.J. Knize, Highly efficient optically pumped cesium vapor laser, Opt. Commun. 260 (2006) 696–698.
[6] M.D. Rotondaro, B.V. Zhdanov, M.K. Shaffer, R.J. Knize, Beam quality measurement of a static-cell cesium DPAL with a stable resonator, Opt. Express 26 (5) (2018) 5497–5500.
[7] S. Wang, J. Han, G. An, W. Zhang, H. Cai, Q. Yu, X. Liu, K. Dai, A. Alghazi, Y. Wang, Demonstration of a dual-wavelength alkali laser with a mixed rubidium–cesium vapor cell, Opt. Commun. 458 (2020), 124758.
[8] B. Sehn, J. Huang, X. Xu, C. Xia, B. Pan, Investigation of pump-to-seed beam matching on output features of Rb and Cs vapor laser amplifiers, Opt. Laser Technol. 101 (2018) 183–188.
[9] F. Gao, F. Chen, J.J. Xie, D.J. Li, L.M. Zhang, G.L. Yang, J. Guo, L.H. Guo, Review on diode-pumped alkali vapor laser, Optik 124 (2013) 4353–4358.
[10] K. Prics, S. Karlsen, P. Leisher, R. Martinsen, High brightness fiber coupled pump laser, Dev., Proc. SPIE 7583 (2010), 758308.
[11] H. Kissel, B. kohler, and J. Biesenbach, High-power diode laser pumps for alkali lasers (DPALs), Proc. of SPIE 8241 (2012) 82410Q.
[12] Z. Yang, H. Wang, Y. Li, Q. Lu, W. Hua, X. Xu, J. Chen, A smile insensitive method for spectral linewidth narrowing on high power laser diode arrays, Opt. Commun. 284 (2011) 5189–5191.
[13] Z.Y. Li, R.Q. Tan, C. Xu, L. Li, Z.L. Zhao, A linearly-polarized rubidium vapor laser pumped by a tunable laser diode array with an external cavity of a temperature-controlled volume bragg grating, Chin. Phys. Lett. 30 (3) (2013), 034202.
[14] Y. Li, V. Negoita, T. Barnowski, S. Strohmaier, and G. Treusch, Wavelength Locking of High-Power Diode Laser Bars by Volume Bragg Gratings, Photonics Society Summer Topical Meeting Series, IEEE (2012).
[15] R. Mcbride, N. Trela, J.J. Wendland, and H.J. Naker, Extending the locking range of VHG-stabilized diode laser bars using wavefront compensator phaseplates Proc. of SPIE 8039 (2011) 80390F.

[16] Z.N. Yang, H.Y. Wang, Q.S. Lu, W.H. Hua, X.J. Xu, An 80-W laser diode array with 0.1 nm linewidth for rubidium vapor laser pumping, Chin. Phys. Lett. 28 (10) (2011), 104202.
[17] R. Pandey, D. Merchen, D. Stapleton, D. Irwin, C. Humble, S. Patterson, H. Kissel, and J. Biesenbach, Narrow-line, tunable, high-power, diode laser pump for DPAL applications, Proc. of SPIE 8733 (2013) 873307.
[18] R. Wang, Z. Yang, H. Tang, L. Li, H. Zhao, H. Wang, X. Xu, A linewidth narrowed diode laser for metastable Argon atom pumping, Opt. Commun. 502 (2022), 127398.
[19] G.J. Steckman, W. Liu, R. Platz, D. Schroeder, C. Moser, Volume holographic grating wavelength stabilized laser diodes, IEEE J. Sel. Top. QUANTUM Electron. 13 (3) (2007) 672–678.
[20] C.H. Henry, Theory of spontaneous emission noise in open resonators and its application to lasers and optical amplifiers, J. Light. Technol. 4 (3) (1986) 288–297.
[21] B. Leonhäuser, H. Kissel, J.W. Tomm, M. Hempel, A. Ungera, and J. Biesenbach, High-Power Diode Lasers under External Optical Feedback, Proc. of SPIE the International Society for Optical Engineering, 9348 (2015).
[22] C. Schnitzler, S. Hambuecker, O. Ruebenach, V. Sinhoff, G. Steckman, L. West, C. Wessling, D. Hoffmann, Wavelength Stabilization of HPDL Array –Fast-Axis Collimation Optic with integrated VHG, Proc. of SPIE 6456 (2007) 645612.
[23] R. Liu, X. Jiang, T. Yang, X. He, Y. Gao, J. Zhu, T. Zhang, W. Guo, B. Wang, Z. Guo, L. Zhang, L. Chen, High brightness 9xxnm fiber coupled diode, Lasers, Proc. SPIE 9348 (2015) 93480V.
[24] S. Yin, B. Zhang, Y. Dan, Effects of the deformation of reflection volume Bragg gratings on the M2-factor of super-Gaussian laser beams, Opt. Commun. 283 (2010) 1418–1423.